Spatially Efficient Design of Annotated Metro Maps

Hsiang-Yun Wu[1], Shigeo Takahashi[1], Daichi Hirono[1], Masatoshi Arikawa[1], Chun-Cheng Lin[2], and Hsu-Chun Yen[3]

[1]The University of Tokyo, Japan
[2]National Chiao Tung University, Taiwan
[3]National Taiwan University, Taiwan

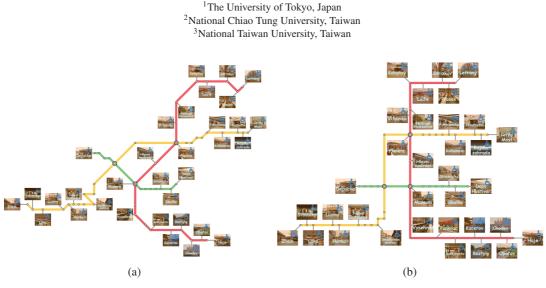(a)   (b)

Figure 1: *Wheelchair accessible stations in Prague metro. (a) Octilinear and (b) orthogonal annotated maps.*

Abstract

Annotating metro maps with thumbnail photographs is a commonly used technique for guiding travelers. However, conventional methods usually suffer from small labeling space around the metro stations, especially when they are interchange stations served by two or more metro lines. This paper presents an approach for aesthetically designing schematic metro maps while ensuring effective placement of large annotation labels that are sufficiently close to their corresponding stations. Our idea is to distribute such labels in a well-balanced manner to labeling regions around the metro network first and then adjust the lengths of metro line and leader line segments, which allows us to fully maximize the space coverage of the entire annotated map. This is accomplished by incorporating additional constraints into the conventional mixed-integer programming formulation, while we devised a three-step algorithm for accelerating the overall optimization process. We include several design examples to demonstrate the spatial efficiency of the map layout generated using the proposed approach through minimal user intervention.

Keywords: Metro maps, annotation labels, efficient space coverage, mixed-integer programming

1. Introduction

Schematic representation of metro maps significantly improves the visual readability of the map contents due to its clear and simplified layout design, especially for guiding complicated metro networks. Currently available metro maps usually follow the aesthetic criteria invented by Beck [Rob03], where the metro lines are aligned to horizon-

tal and vertical directions and optionally 45 degree diagonal directions. In addition, annotating the map with comprehensive explanations and photographs effectively allows us to find sufficient information on our own places of interest. Actually, this type of schematic representation with such large annotation labels has been widely employed in commercially available metro maps and travel guidebooks [Gui12].

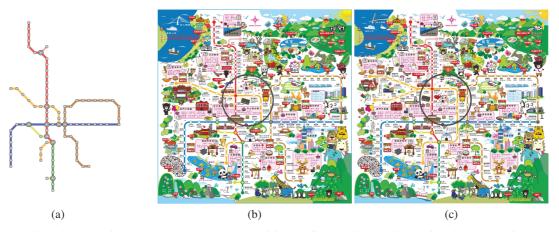<div align="center">(a)   (b)   (c)</div>

Figure 2: *(a) The reference schematic Taipei MRT map. Hand-drawn illustrated maps designed in (b) 2011 and (c) 2012 for "Taipei MRT map handkerchief" (courtesy of Milu Design Co., LTD, Taiwan). Metro line segments circled in gray are elongated after the opening of new lines.*

Nonetheless, the design of such annotated metro maps has not been fully automated so far and thus is often conducted by professional illustrators.

On the other hand, professional illustrators often share common aesthetic criteria in designing the annotated metro maps. Among them, the most primary principle is to apply minimal transformation to the original schematic layout, so that they can spare additional space for placing large annotation labels while making the overall map more compact. Figure 2 presents such an example of Taipei metro map. In practice, the original schematic layout (Figure 2(a)) is successfully incorporated into its annotated version (Figure 2(b)) by locally adjusting the orientations and lengths of metro line segments. Furthermore, this layout has been further revised to rearrange a new version (Figure 2(c)) after new lines are opened, where several metro lines are extended or shrunk to apply local deformations to the entire map layout. Indeed, this observation provides us with an insight into the automatic design of annotated metro maps in our context.

This paper presents a novel approach for aesthetically designing schematic metro maps while ensuring effective placement of large annotation labels that are sufficiently close to their corresponding stations. Our idea is to distribute annotation labels in a well-balanced manner to labeling regions around the metro network first, and then adjust the lengths of metro line segments, so that we can seek the minimal deformation of the entire annotated map to maximize its space coverage. This is accomplished by extending the conventional mixed-integer programming (MIP) formulation for computing schematic layout of metro maps, where we incorporated aesthetic criteria for label placement as additional constraints. The overall computation is further accelerated through a three-step optimization process, by fully taking advantage of the aforementioned design aesthetics commonly employed by map illustrators. Figure 1 shows how our approach can compactly annotate wheelchair acces-

sible stations in Prague metro with large image labels, while applying minimal deformations to the metro network.

The remainder of this paper is structured as follows: Section 2 briefly summarizes related work. Section 3 formulates aesthetic criteria for annotated metro maps together with an overview of the three-step optimization process. The overall process is detailed from Section 4 to Section 6. Section 4 describes a step for computing an initial layout of the metro network. Section 5 presents an extended version of the conventional MIP formulation where additional aesthetic criteria for label annotation have been incorporated in the second step. Section 6 explains how the lengths of metro line segments are adjusted to make the entire annotated map more compact. After having presented several design examples together with discussions in Section 7, we conclude this paper and refer to future work in Section 8.

2. Related Work

In this section, we review two research topics: metro network layout and annotation label placement.

2.1. Metro network layout

The history of the schematic metro map design can be traced back to 1933 when Harry Beck created the first schematic map of the London Underground by introducing several aesthetic design rules [Gar94]. The most important rule is to align metro line segments with one of the octilinear directions, which significantly improves the readability of the map content from a perceptual point of view. Nonetheless, automatically generating such octilinear layouts has been a challenging problem [Gar94, Tuf90, Tuf97]. As reminded in a survey by Wolff [Wol07], the pioneering work of schematic metro map visualization has been done by Hong et al. [HMD05], where they modified the conventional spring-embedder model specifically for drawing metro networks.

Stott et al. [SRMOW11] introduced the hill climbing method to optimize the cost function under constraints derived from multiple aesthetic criteria. The most relevant work is the approach based on mixed-integer programming (MIP) formulated by Nöllenburg et al. [NW11], where they rigorously retain the octilinear layout of the metro network. Wang et al. [WC11] devised an accelerated algorithm through continuous shape smoothing and approximation. Other metro line representations based on adjacency matrices [SM07] and Bézier curves [FHN*13] are also available. However, these conventional methods cannot directly rearrange the layout of annotation labels especially when they are relatively large.

2.2. Annotation label placement

Techniques for placing annotation labels can be categorized into *internal labeling* and *external labeling*. The internal labeling is a method for placing a relatively small label sufficiently close to the corresponding landmark point called *site*. In the external labeling, on the other hand, we usually reserve specific space for placing large annotation labels beforehand while the space is usually far away from the sites. We also connect the label and its corresponding site with a line segment called a *leader* to clarify the correspondence between them. The internal labeling serves as a common technique for annotating point features with small text labels especially in cartographic illustrations. Christensen et al. [CMS95] presented an empirical survey on heuristic algorithms for this purpose, and since then many improved techniques have been intensively investigated [FP99, HAS04, SSB06, Mot07, dE08, BNPW10]. Meanwhile, Bekos et al. proposed a representative technique for the external labeling called *boundary labeling* [BKSW07], where they arranged annotation labels within the margin around the central map content. Their mathematical formulations have also inspired other sophisticated techniques so far [LKY08, BKS08, Lin10, BKNS10, Lin10, WTLY12].

Taking advantage of both the internal and external labels motivates us to seek more effective ways to annotate landmark features with large labels [HGAS05, BKPS11, WTLY11]. Although our previous methods tackled the placement of large annotation labels also, they cannot fully enhance the space coverage of the final annotated maps due to the fixed layout of metro maps [WTLY11] or predefined space allocation for annotation labels [WTLY12]. On the other hand, the proposed approach can be considered as a hybrid of the internal and external labeling techniques, in the sense that we try to place relatively large annotation labels in the vicinity of the corresponding landmark features.

3. System Overview

This section presents an overview of our approach for spatially efficient design of annotated metro maps. Here, we introduce design rules for label placement employed in our approach, followed by the overview of our algorithm.

3.1. Design rules for annotated metro maps

Major criteria for designing schematic layout of the metro network were intensively explored, while, for placing annotation labels, only small textural labels such as station names have been considered so far. However, map annotation with large labels has been already popular among commercially available travel guidebooks since they can assist travelers with rich information about areas of interest. Unfortunately, such maps have been manually composed by professional illustrators only (cf. Figure 2), due to the difficulty in finding visually appealing layout of large annotation labels.

Here, we investigate important criteria for placing large annotation labels to construct an automatic algorithm for generating aesthetic annotated metro maps. Actually, by studying common design rules employed in published guidebooks, we formulate the following criteria as constraints:

(AH1) Leader octilinearity: Align leader line segments along octilinear directions
(AH2) Overlap-free layout: Avoid overlaps among metro lines, annotation labels, and label leaders
(AS1) Leader orientation: Maximize the angles between the leader and its adjacent metro lines
(AS2) Total leader length: Minimize the total leader length
(AS3) Leader bends: Minimize the number of leader bends
(AS4) Closed regions: Avoid placing annotation labels in small regions confined by the metro network
(AS5) Alternating distribution: Distribute annotation labels alternately to incident regions along metro lines

Note that the first two are formulated as *hard* constraints while the last five are as *soft* constraints. In our approach, we introduce these as additional constraints into the conventional MIP formulation [NW11], so that we can seek a reasonable compromise between the aesthetic layout of the metro network and large annotation labels.

3.2. Overview of the algorithm

In an annotated metro map, a set of stations are connected with large annotation labels with leaders, where each leader has one bend at most and thus it can represented as two segments merged at a leader joint. We choose this leader style to seek the best compromise between the degree of freedom in the leader shape and computational complexity of its optimization. Furthermore, this setup lets us represent an annotated metro network as a planar graph $G = (V, E)$, where V and E are the sets of vertices and edges, respectively. Here, $V = V_s + V_j + V_c$ where V_s, V_j, and V_c indicate the sets of the *stations*, *leader joints*, and *label centers*, respectively, and $E = E_m + E_f + E_s$ where E_m, E_f, and E_s correspond to the sets of the *metro line segments*, *first leader line segments* connecting stations and leader joints, and *second leader line segments* connecting leader joints and label centers, respectively. In our approach, it is assumed that at each center ver-
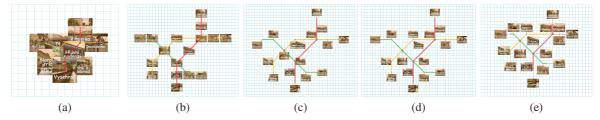
(a)   (b)   (c)   (d)   (e)

Figure 3: *Overview of our algorithm for generating an annotated metro map. (a) An initial layout of the metro network with annotation labels. (b) An enlarged layout by a scale factor of 4. (c) Initial placement of annotation labels having mutual overlaps. (d) Overlap-free placement of annotation labels. (e) Final annotated map after minimal contraction has been applied.*

tex we place the center of rectangular annotation label while we can adaptively adjust its width and height.

In practice, we can design the layout of the annotated metro network all at once using the MIP formulation, while this causes excessive computation time, because a single graph, which represents the entire annotated metro network, has more elements than that for the metro network only, and thus we inevitably suffer from a large number of degrees of freedom in its design. In our approach, we decompose the associated computation into three steps by taking into account the drawing process of professional illustrators as described earlier. Indeed, this significantly reduces computational complexity inherent in the original optimization problem. Although such approximation algorithms may introduce possible infeasibility into the optimization problem, our algorithm usually succeeds in finding visually plausible layouts of the metro network in our setting.

Figure 3 illustrates the overview of the three-step algorithm. We first find an initial schematic layout of the metro network using a variant of the conventional MIP formulation (Figure 3(a)). After having enlarged the initial layout by some scale factor (Figure 3(b)), we seek a well-balanced distribution of annotation labels to regions around the network while adjusting the lengths and orientations of the label leaders (Figures 3(c) and (d)). Here, the scale factor is proportionally adjusted according to the size of the largest annotation labels to be placed. Finally, we compute an optimized layout of the annotated metro map by contracting the metro line segments so that we can tightly enclose the annotation labels with the metro network (Figure 3(e)). Note that we have to avoid mutual overlaps between the edges and annotation labels during this process. In our approach, we repeatedly resolve overlaps between these map elements in each optimization process until we can obtain an overlap-free layout. These steps will be detailed in the following three sections.

4. Initializing the Metro Network Layout

This section describes how we find an initial layout of the metro network, which serves as a basis for further placing rectangular labels around it. For this purpose, we compute schematic layouts of the metro networks by introducing the
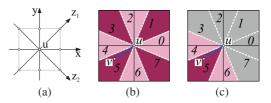

(a)   (b)   (c)

Figure 4: *Aligning metro lines with octilinear directions. (a) Octilinear coordinate system around the vertex u, where $z_1(u) = (x(u) + y(u))/2$ and $z_2(u) = (x(u) - y(u))/2$. (b) The corresponding fan-shaped sectors with respect to u. (c) Three sectors to which the optimized version of $\overline{uv}$ belongs.*

MIP formulation [NW11], where we incorporate a set of new constraints to better control the shape of the metro network.

4.1. Mixed-integer programming

The conventional MIP formulation [NW11] allows us to place all the stations on the integer grid coordinates, and rigorously align every metro line segment to one of the octilinear directions by referring to the horizontal, vertical, and 45 degree diagonal axes (Figure 4(a)). This is accomplished by classifying the corresponding edge segment to one of the eight fan-shaped sectors (Figure 4(b)), where the orientation of the edge $\overline{uv}$ falls into the sector 5, for example. In the conventional MIP formulation, we achieve this embedding by minimizing the following linear objective function:

$$w_{(LS1)}\text{cost}_{(LS1)} + w_{(LS2)}\text{cost}_{(LS2)} + w_{(LS3)}\text{cost}_{(LS3)}, \quad (1)$$

$$\text{cost}_{(LS1)} = \sum_{uvw \in L_t} \text{bd}(u, v, w), \quad (2)$$

$$\text{cost}_{(LS2)} = \sum_{uv \in E_m} \text{rpos}(uv), \quad (3)$$

$$\text{cost}_{(LS3)} = \sum_{uv \in E_m} \lambda(uv). \quad (4)$$

Here, L_t represents the set of adjacent two edges on a metro line while E_m is the set of metro line segments as described earlier. Furthermore, $\text{cost}_{(LS1)}$ penalizes the amount of the bend $\text{bd}(u, v, w)$ by referring to the angle spanned by $\overline{vu}$ and $\overline{vw}$, $\text{cost}_{(LS2)}$ lets us preserve the original directions of the network edges by computing $\text{rpos}(uv)$, i.e., the difference between the original sector number of $\overline{uv}$ and its optimized one, and $\text{cost}_{(LS3)}$ is used to minimize the sum of $\lambda(uv)$, the length of the edge $\overline{uv}$, for finding a tight layout of the metro network. Note that $w_{(LS1)}$, $w_{(LS2)}$, and $w_{(LS3)}$ are the weights

for the three cost terms, respectively. Refer to [NW11] for this notation, which we also employed in this paper.

4.2. Computing nearly orthogonal layouts

As well as the octilinear layouts, we compute nearly orthogonal layouts of the metro network as an option. This helps us to pack rectangular labels more tightly into the available labeling space. We achieve this by slightly modifying the conventional MIP formulation. Actually, the conventional formulation limits every edge to fall into one of the *preceding*, *original*, and *succeeding* sectors, and penalizes Eq. (3) if the optimized edge goes out of the original sector. In Figure 4(c), for example, the original sector of $\overline{uv}$ is encoded as 5 while its corresponding preceding and succeeding sectors are 4 and 6, respectively. For computing the nearly orthogonal layout for our purpose, we penalize Eq. (3) when the optimized edge is distributed to diagonal sectors irrespective of the sector to which the original edge belongs.

5. Spatially-Efficient Placement of Annotation Labels

This section describes how to formulate the aesthetic placement of large annotation labels as a MIP model, which is the primary contribution of this paper. Note that in this second step, we first enlarge the initial layout of the metro network in order to spare sufficient labeling space around it, and then try to embed large annotation labels together with their leaders, by following the aesthetic criteria described in Section 3. The main challenge here is to formulate such aesthetic criteria as linear constraints for the MIP model, while seeking a reasonable compromise between the aesthetic layout of the metro network and annotation labels. For this purpose, we minimize the sum of five cost terms as follows:

$$\sum_{i=1}^{5} w_{(ASi)} \text{cost}_{(ASi)}, \quad (5)$$

where $w_{(AS1)}, \ldots, w_{(AS5)}$ represent the weights for the five cost terms, respectively. Here, these cost terms correspond to the five soft constraints listed in Section 3.1. The remainder of this section describes how we formulated each of the two hard constraints and five soft constraints described earlier.

5.1. Label leader styles

First of all, we employ the styles of label leaders as shown in Figure 5(a), for preserving the *leader octilinearity* (AH1). Here, each leader line consists of two line segments in such a way that the *first* segment connects the *station* vertex v and *joint* vertex j and the *second* segment bridges j and the *label center* vertex p. Note that the leader joint and label center vertices are located at the integer grid coordinates again in our formulation. We also align the first leader segment (in the area shaded in gray) with one of the octilinear directions while keeping its L_1-norm to be proportional to the size of annotation label, as described later. The orientation of the

second leader segment (in the area shaded in red), on the other hand, is restricted to horizontal and vertical while its length can be extended freely to some extent. Thus, we have twelve leader types (i.e. E, NEE, NEN, N, NWN, NWW, W, SWW, SWS, S, SES, and SEE) in total. This leader style setup provides us with appropriate degrees of freedom in their shapes as well as the capability to fit the corresponding annotation labels more compact to the available space. In practice, these label leader styles are often employed in published maps also.

5.2. Leader orientation

To avoid any undesirable visual clutter between the metro lines and leader lines, we would like to adjust the orientation of each first leader segment using *leader orientation* (AS1) constraints so that it makes a maximal angle with the metro line segments that share the same station vertex v (Figure 5(b)). Given a leader edge $\overline{vj}$ and a metro network edge $\overline{vu}$, we can penalize the similarity in orientation between the two edges by introducing a new variable $\text{ls}(u,v,j)$ as:

$$\min\{|\text{dir}(v,u) - \xi|, 8 - |\text{dir}(v,u) - \xi|\} = 4 - \text{ls}(u,v,j). \quad (6)$$

Here, $\text{dir}(v,u)$ represents the edge sector of $\overline{vu}$ and ξ corresponds to the sector of the first leader segment $\overline{vj}$. Eq. (6) follows from the fact that the octilinear sector ranges from 0 to 7 and circulates in that range, which means that the difference in sector is $|\text{dir}(v,u) - \xi|$ or $8 - |\text{dir}(v,u) - \xi|$ and its upper limit is 4. According to the sign of the absolute value in Eq. (6), we can rewrite the above condition as:

$$\sigma_0(v) + \sigma_1(v) + \sigma_2(v) + \sigma_3(v) = 1 \quad (7)$$

$$\begin{aligned}
\text{dir}(v,u_i) - \xi &\leq M(1 - \sigma_0(v)) + 4 - \text{ls}(u,v,j) \\
\text{dir}(v,u_i) - \xi &\geq -M(1 - \sigma_0(v)) + 4 - \text{ls}(u,v,j) \\
-\text{dir}(v,u_i) + \xi &\leq M(1 - \sigma_1(v)) + 4 - \text{ls}(u,v,j) \\
-\text{dir}(v,u_i) + \xi &\geq -M(1 - \sigma_1(v)) + 4 - \text{ls}(u,v,j) \\
-\text{dir}(v,u_i) + \xi &\leq M(1 - \sigma_2(v)) - 4 - \text{ls}(u,v,j) \\
-\text{dir}(v,u_i) + \xi &\geq -M(1 - \sigma_2(v)) - 4 - \text{ls}(u,v,j) \\
\text{dir}(v,u_i) - \xi &\leq M(1 - \sigma_3(v)) - 4 - \text{ls}(u,v,j) \\
\text{dir}(v,u_i) - \xi &\geq -M(1 - \sigma_3(v)) - 4 - \text{ls}(u,v,j)
\end{aligned} \quad (8)$$

where $\sigma_i(v)(i = 0, \ldots, 3)$ are new binary variables that are introduced to validate two of the eight inequalities in Eq. (8), and M corresponds to a large value used to retain inequality constraints when the corresponding $\sigma_i(v)$ vanishes [NW11]. The cost term $\text{cost}_{(AS1)}$ can be obtained by accumulating the absolute difference between two variables, for example, $\text{ls}(u,v,j)$ and $\text{ls}(w,v,j)$, where $\overline{vu}$ and $\overline{vw}$ are edges incident to v and are adjacent to each other around v. Thus, we obtain:

$$-\text{diff}(u,v,w,j) \leq \text{ls}(u,v,j) - \text{ls}(w,v,j) \leq \text{diff}(u,v,w,j) \quad (9)$$

$$\text{cost}_{(AS1)} = \sum_{v \in V_s, \overline{vj} \in E_f, \overline{vu}, \overline{vw} \in E_m} \text{ls}(u,v,j) + \text{ls}(w,v,j) + \text{diff}(u,v,w,j). \quad (10)$$

Note that this term lets us align the first leader segment close to the bisector of the largest angle spanned by metro edges.
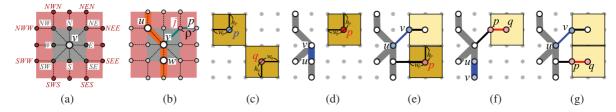
Figure 5: *Aesthetic constraints for spatially-efficient map design. (a) Twelve leader styles. (b) Aligning a leader line to make a maximal angle with adjacent metro lines. Checking overlap between (c) two labels, (d) a label and a metro line segment, (e) a label and a leader line segment, (f) leader and metro line segments, and (g) two leader line segments.*

5.3. Leader octilinearity and total leader length

We formulate the *leader octilinearity* (**AH1**) and *total leader length* (**AS2**) constraints together in this section. Suppose that we consider the leader vjp, where v, j, and p correspond to a station, a leader joint, and a label center, respectively. We encode the orientation of the first leader segment $\overline{vj}$ by

$$\sum_{i \in \{N,S,E,W,NE,NW,SE,SW\}} \tau_i = 1 \qquad (11)$$

using new binary variables τ_i, which satisfy:

$$\xi = 0 \cdot \tau_E + 1 \cdot \tau_{NE} + \cdots + 7 \cdot \tau_{SE}. \qquad (12)$$

Now let us encode the leader styles of the type *NEE* and *NEN*, by considering the orientation of the first and second leader segments $\overline{vj}$ and $\overline{jp}$, respectively, (Figure 5(a)) as:

$$
\begin{aligned}
\tau_{NE} = \tau_{NEE} + \tau_{NEN} \\
-2M(1-\tau_{NE}) + B \le x(j) + y(j) - x(v) - y(v) \\
\le 2M(1-\tau_{NE}) + B \\
-2M(1-\tau_{NE}) \le x(j) - y(j) - x(v) + y(v) \\
\le 2M(1-\tau_{NE}) \\
x(p) - x(j) \ge -M(1-\tau_{NEE}) + K \\
-M(1-\tau_{NEE}) \le y(p) - y(j) \le M(1-\tau_{NEE}) \\
y(p) - y(j) \ge -M(1-\tau_{NEN}) + K \\
-M(1-\tau_{NEN}) \le x(p) - x(j) \le M(1-\tau_{NEN}) \\
\vdots
\end{aligned} \qquad (13)
$$

where τ_{NEE} and τ_{NEN} are again binary variables that become true if $\overline{jp}$ coincides with the corresponding orientation. The constant B represents the predefined length of the first leader segment $\overline{vj}$ as describe earlier, and is set to be half the sum of the width and height of the corresponding rectangular label by default. On the other hand, the second leader segment $\overline{jp}$ has the lower limit length K (set to be 0 by default) and is minimized by penalizing:

$$\text{cost}_{(AS2)} = \sum_{jp \in E_s} \rho(j,p). \qquad (14)$$

where $\rho(j,p)$ represents the length of $\overline{jp}$ and satisfies:

$$
\begin{aligned}
-\rho(j,p) &\le x(j) - x(p) \le \rho(j,p) \\
-\rho(j,p) &\le y(j) - y(p) \le \rho(j,p).
\end{aligned} \qquad (15)
$$

5.4. Leader bends

The *leader bends* (**AS3**) constraint is formulated by introducing an additional variable lbd for each leader vjp, so that
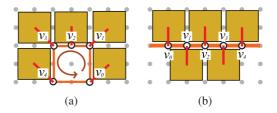

Figure 6: *Distributing annotation labels to incident regions. (a) Labels are kicked out of a small closed region. (b) Labels are placed alternately to incident regions along a metro line.*

we penalize the case where the first segment $\overline{vj}$ is aligned with a diagonal direction since, in that case, the leader always has a bend at the joint j (Figure 5(a)). This implies that $\text{lbd}(p,j,v) = \tau_{NE} + \tau_{NW} + \tau_{SW} + \tau_{SE}$. Thus, we obtain:

$$\text{cost}_{(AS3)} = \sum_{v \in V_s, vj \in E_f, jp \in E_s} \text{lbd}(p,j,v) \qquad (16)$$

5.5. Closed regions

In general, we should avoid inserting annotation labels into small regions that are completely enclosed by the metro network (Figure 6(a)). This is because such annotation labels become obstacles when we contract metro line segments to make the overall map more compact in the last step. In our approach, we alleviate this problem by introducing the *closed region* (**AS4**) constraints, which penalize the number of labels confined in each closed region. For later convenience, we also partition the map domain by extending each metro line, which leads to a dead-end, to the domain boundary so as to identify open regions around the metro network.

Here, we define a binary variable $f_j(v)$ that specifies if the label at the vertex v stays in the j-th region, by referring to the orientation of the corresponding first leader segment, as

$$f_j(v) = c_E \tau_E + c_S \tau_S + \cdots + c_{SW} \tau_{SW}, \qquad (17)$$

where c_i is a *constant* binary value and becomes 1 if the first leader segment is directed toward that region; otherwise it is 0. We can then count labels assigned to that region as:

$$N(f_j) = \sum_{v \in V_s} f_j(v) \qquad (18)$$

Thus, the total number of labels in closed regions is:

$$\text{cost}_{(AS4)} = \sum_{j \in I_c} N(f_j), \qquad (19)$$

where I_c denotes the indices of closed labeling regions.

5.6. Alternating distribution

An important design rule for making the annotated map spatially compact is to distribute annotation labels alternately to incident regions along each metro lines. (See [Tra12] for example.) This is aesthetically reasonable especially for large annotation labels because with constraints of this type we can distribute annotation labels rather uniformly over the map (Figure 6(b)). In our approach, we formulate an *alternating distribution* (**A5**) constraint as:

$$
\begin{aligned}
2a_i &\leq 1 + f_j(v_i) - f_j(v_{i+1}) \leq 1 + a_i \\
2b_i &\leq 1 - f_j(v_i) + f_j(v_{i+1}) \leq 1 + b_i \\
1 - \mathrm{adj}_i(f_j) &\leq \quad a_i + b_i \quad \leq 2(1 - \mathrm{adj}_i(f_j))
\end{aligned}
\tag{20}
$$

where a_i and b_i are newly introduced binary variables and $\mathrm{adj}_i(f_j)$ $(i = 1, \ldots, n)$ are binary variables that penalize the case where two annotation labels, whose corresponding vertices v_i and v_{i+1} are next to each other, are distributed to the same region f_j. Indeed, Eq. (20) computes the XOR of $f_j(v_i)$ and $f_j(v_{i+1})$. Thus, the corresponding cost term is given by

$$
\mathrm{cost}_{(\mathrm{AS5})} = \sum_{j \in I_f} \mathrm{adj}(f_j). \tag{21}
$$

5.7. Overlap-free layout

As described in Section 3, we examine overlaps between map elements such as metro line segments, leader segments, and rectangular labels once we optimize the layout of annotated metro maps, and newly incorporate the corresponding *overlap-free layout* (**AH2**) constraints to our MIP model. This incremental insertion of constraints makes our optimization much faster when compared with the case where an appropriate set of overlap-free constraints is introduced from the beginning. The overlap-free constraints are grouped into three categories: box-box, box-edge, and edge-edge constraints, and can be formulated by referring to [NW11].

Box-Box constraints: Constraints of this type are employed to avoid overlaps between annotation labels as shown in Figure 5(c), and can be formulated as:

$$
\sum_{i \in \{N,S,E,W\}} \mu_i \geq 1 \tag{22}
$$

$$
\begin{aligned}
x(p) - x(q) &\geq w_p + w_q - M(1 - \mu_E) \\
-x(p) + x(q) &\geq w_p + w_q - M(1 - \mu_W) \\
y(p) - y(q) &\geq h_p + h_q - M(1 - \mu_N) \\
-y(p) + y(q) &\geq h_p + h_q - M(1 - \mu_S)
\end{aligned}
\tag{23}
$$

where p and q are label centers, and w_p, w_q, h_p, and h_q are the half widths and heights of two rectangular labels p and q, respectively. Note that we introduce new binary variables μ_i to make one of the four conditions in Eq. (23) hold.

Box-edge constraints: Constraints of this type allow us to check overlaps of annotation labels with metro lines (Figure 5(d)) and leader lines (Figure 5(e)). The overlap-free constraint for the box center p and edge $\overline{uv}$ is given by:

$$
\sum_{i \in \{N,S,E,W,NE,NW,SE,SW\}} \kappa_i \geq 1 \tag{24}
$$

$$
\begin{aligned}
x(p) - x(v) &\geq -M(1 - \kappa_E) + w_p \\
x(p) - x(u) &\geq -M(1 - \kappa_E) + w_p \\
&\vdots
\end{aligned}
\tag{25}
$$

where κ_i are new binary variables for avoiding overlaps between the two elements along all the octilinear direction.

Edge-edge constraints: Edge-edge constraints can be used to resolve overlaps of a leader line with a metro line (Figure 5(f)) and another leader line (Figure 5(g)). The constraint can be formulated between the edges $\overline{pq}$ and $\overline{uv}$ as

$$
\sum_{i \in \{N,S,E,W,NE,NW,SE,SW\}} \chi_i \geq 1 \tag{26}
$$

$$
\begin{aligned}
x(p) - x(u) &\geq -M(1 - \chi_E) + D \\
x(p) - x(v) &\geq -M(1 - \chi_E) + D \\
x(q) - x(u) &\geq -M(1 - \chi_E) + D \\
x(q) - x(v) &\geq -M(1 - \chi_E) + D \\
&\vdots
\end{aligned}
\tag{27}
$$

where χ_i are new binary variables for finding overlap-free placement of the two edge segments. Note that the constant D is set to be 1 by default in our implementation.

6. Contracting Edges of the Metro Network

In the last step of our optimization algorithm, we fix the orientation of the label leaders obtained in the previous step and then adjust the lengths of metro line segments together with the lengths of the second leader line segments. This allows us to find an appropriate deformation for making the entire annotated metro map more spatially compact. We achieve this deformation by fixing all the variables except for $\lambda(uv)$ in Eq. (4) and $\rho(v)$ in Eq. (15) in our MIP model. Thus the objective cost function to be minimized in this step becomes:

$$
w'_{(\mathrm{LS3})} \mathrm{cost}_{(\mathrm{LS3})} + w'_{(\mathrm{AS2})} \mathrm{cost}_{(\mathrm{AS2})}, \tag{28}
$$

where we assign different weight values $w'_{(\mathrm{LS3})}$ and $w'_{(\mathrm{AS2})}$ to the two cost terms, respectively. Indeed, we assign a larger value to $w'_{(\mathrm{AS2})}$ so that we can avoid unnaturally long leader lines in the finalized map layout. Note also that the variables τ_i in Eq. (13) have also been fixed and thus we can reduce the number of linear constraints by substituting for τ_i the binary values we obtained in the second step.

7. Results and Evaluation

Our algorithm was implemented on a desktop PC with two Quad-Core Intel Xeon CPUs (2.4GHz, 12MB cache) and 8GB RAM, and the source code was written in C++ using IBM ILOG CPLEX for solving MIP problems. Figure 1

(a)   (b)   (c)
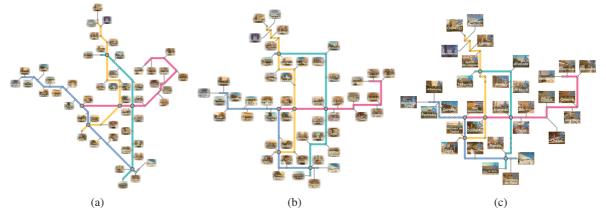
Figure 7: *Lisbon annotated metro maps. (a) Octilinear, (b) orthogonal, and (c) wheelchair accessible stations annotated only.*
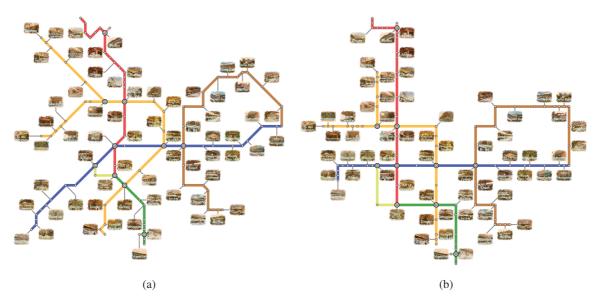

(a)   (b)

Figure 8: *Taipei gourmet metro maps. (a) Octilinear layout. (b) Orthogonal layout.*

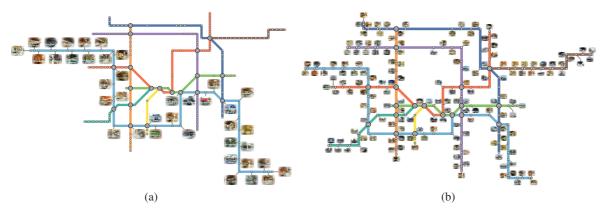(a)   (b)

Figure 9: *Berlin annotated metro maps. (a) Light blue line annotated in an octilinear layout. (b) All the stations annotated in an orthogonal layout.*

shows Prague metro maps where wheelchair accessible stations are selectively annotated with thumbnail photographs, while Figures 1(a) and (b) are in octilinear and orthogonal layouts, respectively. Figures 7(a) and (b) present Lisbon metro maps in the octilinear and orthogonal layouts, respectively, where all the stations are annotated with image labels that are sufficiently close to the corresponding stations. On the other hand, in Figure 7(c), wheelchair accessible stations are only selected to be annotated on the orthogonal layout. Our observation suggests that the orthogonal layouts are more likely to enhance the spatial efficiently of the metro map since annotation labels can be fit more tightly to horizontal and vertical metro lines. Table 1 shows computation times required for automatically generating the aforementioned annotated metro maps. Note that we empirically employ $w_{(LS1)} = 1$, $w_{(LS2)} = 50$, and $w_{(LS3)} = 10$ for the weights in the first step, $w_{(AS1)} = 5$, $w_{(AS2)} = 1$, $w_{(AS3)} = 2$, $w_{(AS4)} = 10$ and $w_{(AS5)} = 100$ in the second step, and $w_{(LS3)} = 1$ and $w_{(AS2)} = 10$ in the third step, respectively.

We also equipped our prototype system with an interface for editing the styles of annotation labels as well as selecting/deselecting stations to be annotated. This selection functionality also allows us to decompose the entire map into smaller areas and edit annotations area by area from dense downtown including interchange stations to sparse suburbs. We accomplish this selective design of label annotation by relaxing MIP variables contained in the target area while keeping other variables to be constant. Figure 8 shows such a design example where Taipei gourmet maps are interactively composed using our system within 30 minutes, where we selectively annotated stations where famous restaurants are located. We can see that the layout of the metro network has been aesthetically transformed for both in the octilinear and orthogonal layouts to make the entire maps more spatially efficient. Figure 9(a) presents a Berlin annotated metro map where we spent 30 minutes or less to interactively annotate stations on a specific route. Here, the effect of map deformation in the final step is the most obvious in the sense that the route together with the associated annotation labels dominates large space of the metro map. Figure 9(b) shows the same metro network while we annotated all stations this time. Of course, scalability is still one of the most significant issues in our approach. However, we can still edit large-sized annotated metro maps by properly partitioning the network into several areas within an hour, as shown in Figure 9(b).

In order to assess the validity of the seven aesthetic criteria described in Section 3.1, we organize a comparative study. We prepared an online questionnaire for this purpose, and incorporated Prague and Vienna metro maps as test examples. For each map, we asked participants to answer seven questions by choosing one of two map images, where one image satisfies one of the seven criteria and the other does not. We recruited 70 participants including 19 females and 51 males aged from 20 to 55. Table 2 shows percentages of positive responses for each of the seven criteria. This result

Table 1: *Computation times (in seconds) for automatically generating annotated metro maps (averaged over 5 trials).*

	Fig 1(a)	Fig 1(b)	Fig 7(a)	Fig 7(b)	Fig 7(c)
1st step	0.13	0.78	2.82	2.16	2.16
2nd step	72.00	23.23	81.70	65.22	2.35
3rd step	163.37	69.84	201.94	87.89	49.22

Table 2: *Percentages of positive responses for each design criterion through online questionnaires.*

City	(AH1)	(AH2)	(AS1)	(AS2)	(AS3)	(AS4)	(AS5)
Prague	80%	100%	67%	74%	50%	67 %	71 %
Vienna	84%	100%	90%	76%	81%	79 %	74 %

ensures that it is reasonable to formulate **(AH1)** and **(AH2)** as hard constraints since the corresponding percentages are quite high. We also handle other criteria as soft constraints because they may conflict with each other. This means that we do not rigorously optimize each criteria, but rather try to seek the best compromise among them by adjusting the weight values associated with each cost term (cf. Section 5).

8. Conclusion

This paper has presented an approach to designing spatially efficient annotated metro maps by introducing additional constraints to the conventional MIP formulation. Our approach ensures the effective placement of large annotation labels that are sufficiently close to the landmark stations, while maximizing the space coverage of the map contents through an appropriate deformation of the map layout. We also devised the three-step algorithm for finding feasible solutions within an acceptable period of time, by reasonably restricting the degrees of freedom in the layout of the annotated metro network. An interface for editing the layout of annotated metro maps is provided for users to design their own customized metro maps according to their preference.

Our future work includes the development of more powerful interfaces for fully facilitating the design of annotated metro maps even for naïve users. Implementing our map visualization on mobile devices may demand several new schematization rules of metro lines and annotation labels. Animating annotated metro maps is also a challenging technical problem for future research because we have to retain frame-to-frame temporal coherence for the sake of better map readability. It is also interesting to extend our approach to 3D geographical maps where we can embed more annotation labels into 2D projections of the target 3D scenes.

References

[BKNS10] BEKOS M. A., KAUFMANN M., NÖLLENBURG M., SYMVONIS A.: Boundary labeling with octilinear leaders. *Algorithmica 57*, 3 (2010), 436–461.

[BKPS11] BEKOS M. A., KAUFMANN M., PAPADOPOULOS D., SYMVONIS A.: Combining traditional map labeling with boundary labeling. In *Proceedings of the 37th International Conference on Current Trends in Theory and Practice of Computer Science (SOFSEM2011)* (2011), vol. 6543 of *Springer Lecture Notes in Computer Science*, pp. 111–122.

[BKS08] BEKOS M. A., KAUFMANN M., SYMVONIS A.: Efficient labeling of collinear sites. *Journal of Graph Algorithms and Applications 12*, 3 (2008), 357–380.

[BKSW07] BEKOS M. A., KAUFMANN M., SYMVONIS A., WOLFF A.: Boundary labeling: Models and efficient algorithms for rectangular maps. *Computational Geometry: Theory and Applications 36*, 3 (2007), 215–236.

[BNPW10] BEEN K., NÖLLENBURG M., POON S.-H., WOLFF A.: Optimizing active ranges for consistent dynamic map labeling. *Computational Geometry: Theory and Applications 43*, 3 (2010), 312–328.

[CMS95] CHRISTENSEN J., MARKS J., SHIEBER S.: An empirical study of algorithms for point-feature label placement. *ACM Transactions on Graphics 14*, 3 (1995), 203–232.

[dE08] DO NASCIMENTO H. A. D., EADES P.: User hints for map labeling. *Journal of Visual Languages and Computing 19* (2008), 39–74.

[FHN∗13] FINK M., HAVERKORT H., NÖLLENBURG M., ROBERTS M., SCHUHMANN J., WOLFF A.: Drawing metro maps using Bézier curves. In *Proceedings of the 20th International Symposium on Graph Drawing* (2013), vol. 7704 of *Springer Lecture Notes in Computer Science*, pp. 463–474.

[FP99] FEKETE J.-D., PLAISANT C.: Excentric labeling:dynamic neighborhood labeling for data visualization. In *Proceedings of the SIGCHI conference on Human factors in computing systems* (1999), pp. 512–519.

[Gar94] GARLAND K.: *Mr. Beck's Underground Map: A History*. Capital Transport, 1994.

[Gui12] Visitors guide and bus route map of London. Transport for London, 2012. http://www.tfl.gov.uk/assets/downloads/visitor-guide.pdf.

[HAS04] HARTMANN K., ALI K., STROTHOTTE T.: Floating labels: Applying dynamic potential fields for label layout. In *Proceedings of the 4th International Conference on Smart Graphics (SG2004)* (2004), pp. 101–113.

[HGAS05] HARTMANN K., GOTZELMANN T., ALI K., STROTHOTTE T.: Metrics for functional and aesthetic label layouts. In *Proceedings of the 5th International Symposium on Smart Graphics (SG2005)* (2005), vol. 3638 of *Springer Lecture Notes in Computer Science*, pp. 115–126.

[HMD05] HONG S.-H., MERRICK D., DO NASCIMENTO H. A. D.: The metro map layout problem. In *Proceedings of the 12th International Symposium on Graph Drawing* (2005), vol. 3383 of *Springer Lecture Notes in Computer Science*, pp. 482–491.

[Lin10] LIN C.-C.: Crossing-free many-to-one boundary labeling with hyperleaders. In *Proceeding of the IEEE Pacific Visualization Symposium* (2010), pp. 185–192.

[LKY08] LIN C.-C., KAO H.-J., YEN H.-C.: Many-to-one boundary labeling. *Journal of Graph Algorithm and Appplications 12*, 3 (2008), 319–356.

[Mot07] MOTE K.: Fast point-feature label placement for dynamic visualizations. *Information Visualization 6* (2007), 249–260.

[NW11] NÖLLENBURG M., WOLFF A.: Drawing and labeling high-quality metro maps by mixed-integer programming. *IEEE Transactions on Visualization and Computer Graphics 17*, 5 (2011), 626–641.

[Rob03] ROBERTS M. J.: *Underground Maps After Beck*. Capital Transport, 2003.

[SM07] SHEN Z., MA K.-L.: Path visualization for adjacency matrices. *Computer Graphics Forum* (2007), 83–90.

[SRMOW11] STOTT J., RODGERS P., MARTINEZ-OVANDO J. C., WALKER S. G.: Automatic metro map layout using multicriteria optimization. *IEEE Transactions on Visualization and Computer Graphics 17*, 1 (2011), 101–114.

[SSB06] STADLER G., STEINER T., BEIGLBÖCK J.: A practical map labeling algorithm utilizing morphological image processing and force-directed methods. *Cartography and Geographic Information Science 33*, 3 (2006), 207–215.

[Tra12] Tramlink network map. Transport for London., 2012. http://www.tfl.gov.uk/assets/downloads/tramlink-network-map.jpg.

[Tuf90] TUFTE E. R.: *Envisioning Information*. Graphics Press LLC, 1990.

[Tuf97] TUFTE E. R.: *Visual Explanations: Images and Quantities, Evidence and Narrative*. Graphics Press LLC, 1997.

[WC11] WANG Y.-S., CHI M.-T.: Focus+context metro maps. *IEEE Transactions on Visualization and Computer Graphics 17*, 12 (2011), 2528–2535.

[Wol07] WOLFF A.: Drawing subway maps: A survey. *Informatik - Forschung und Entwicklung 22* (2007), 23–44.

[WTLY11] WU H.-Y., TAKAHASHI S., LIN C.-C., YEN H.-C.: A zone-based approach for placing annotation labels on metro maps. In *Proceedings of the 11th International Conference on Smart Graphics (SG2011)* (2011), vol. 6815 of *Springer Lecture Notes in Computer Science*, pp. 91–102.

[WTLY12] WU H.-Y., TAKAHASHI S., LIN C.-C., YEN H.-C.: Travel-route-centered metro map layout and annotation. *Computer Graphics Forum 31*, 3 (2012), 925–934.